Monitoring fluence of neutrons for investigation radiation hardness of detectors and electronics in NPI of ACSR

NPI Rez:V. Kushpil, A. Kugler, S. Kushpil, O. Svoboda

JINR: V. Ladygin, A.Khrenov, S.Piyadin, S.Reznikov, A.Yu.Isupov

Neutrons – new factor for modern experiments

NA61 Projectile Spectator Detector

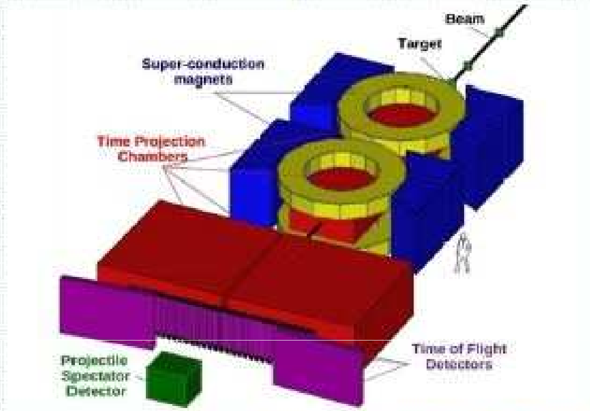

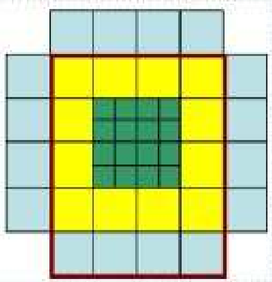

60 sandwiches in one module
16 inner modules of 10 x 10 x 120 cm^3
28 outer modules of 20 x 20 x 120 cm^3
Total weight ~ 17 tons, 17-25 m from target
No beam hole for intensity up to $2x10^5$ ions/sec
NA61 beam energy up to 150 AGeV

NICA MPD Zero Degree Calorimeter

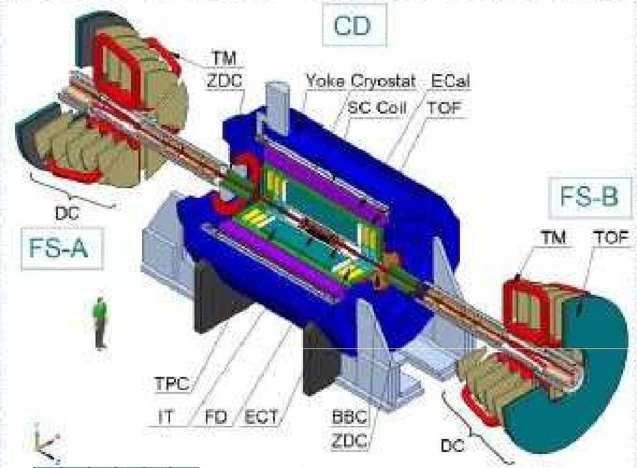

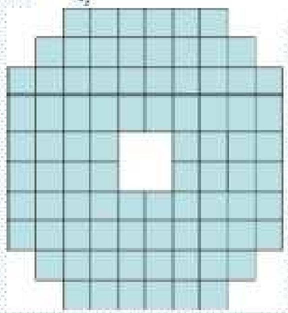

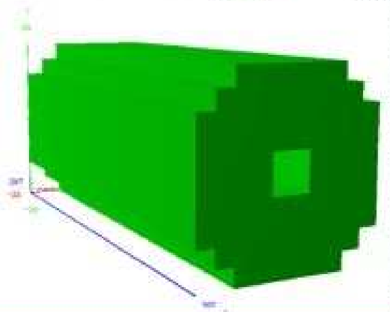

60 sandwiches in one module
16 modules of 5 x 5? x 120 cm^3
Total weight ~ 10 tons, 28 m from collision estimate
Beam hole (10x10 cm) for intensity up to $1x10^9$??? ions/sec
NICA beam energy up to $\sqrt{s_{NN}}$ =11GeV?(~ E_{beam}=63 AGeV)

CBM-PSD simulations

The PSD detector from CBM will be used to explain basic goals of program:

From geometry of PSD we can see that neutrons is most important type of particles which will define radiation hardness of APD.

The simulation show that this is true supposed

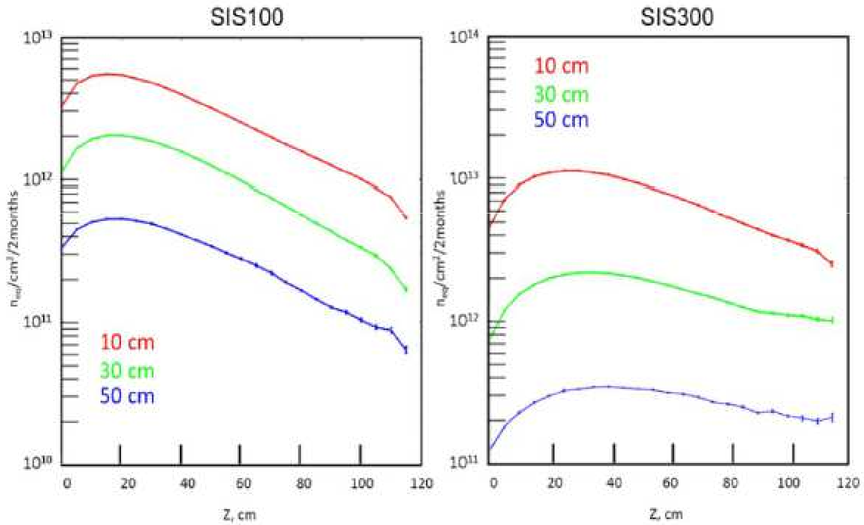

Distributions of the neutron flux (n/cm2/s) through the PSD calorimeter at radius 10, 30 and 50 cm

FLUKA simulation results:
Flux near the beam hole after 2 months of CBM run at the beam rate 10^8 ions/s:

10^{12} n/cm2 for E_{beam}(Au) 4 AGeV

4×10^{12} n/cm2 for E_{beam}(Au) 35 AGeV

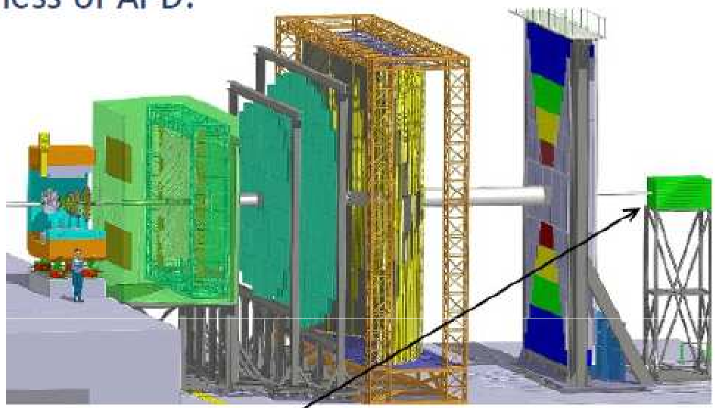

Projectile Spectator Detector for CBM experiment

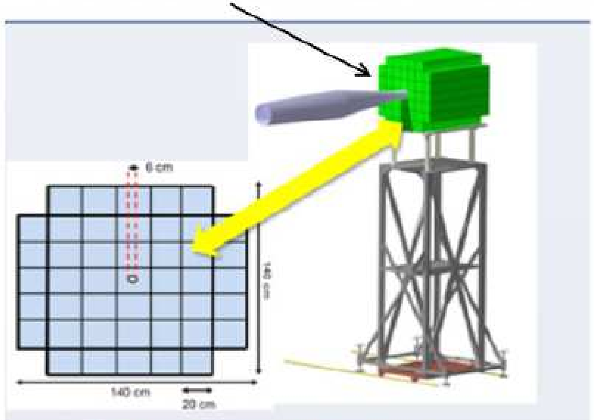

PSD with the reduced beam hole

U120 and neutrons sources

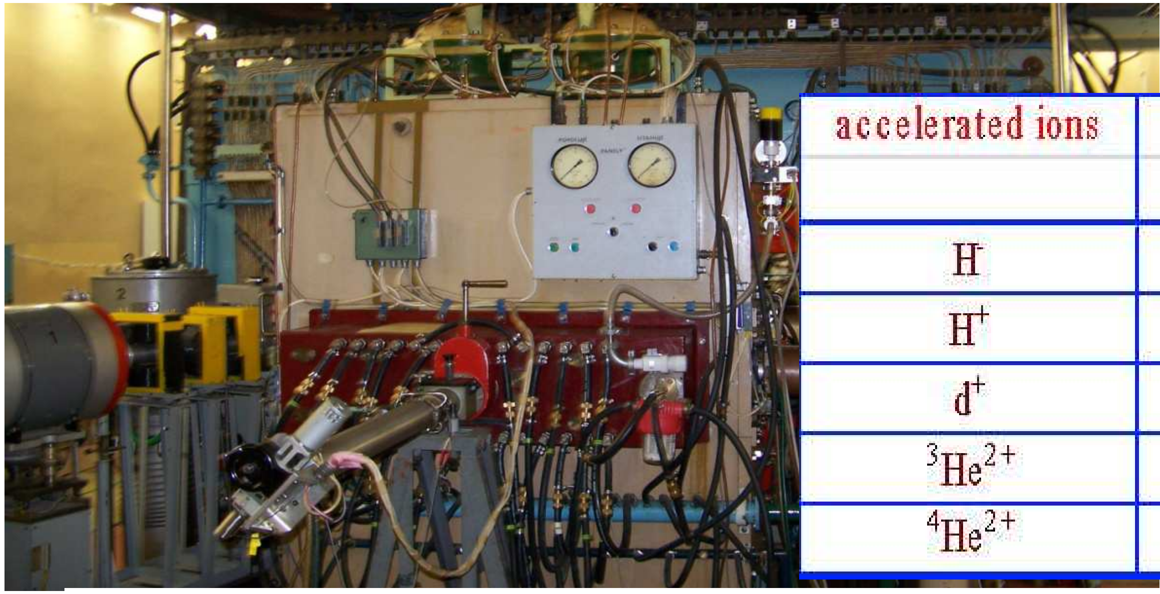

accelerated ions	energy [MeV]	extracted currents [μA]
H^-	6 - 38	15 - 35
H^+	6 - 38	3
d^+	11 - 20	3
$^3He^{2+}$	16 - 55	3
$^4He^{2+}$	22 - 40	3

Quasi-monoenergetic neutron beam by ^{7}Li(C)

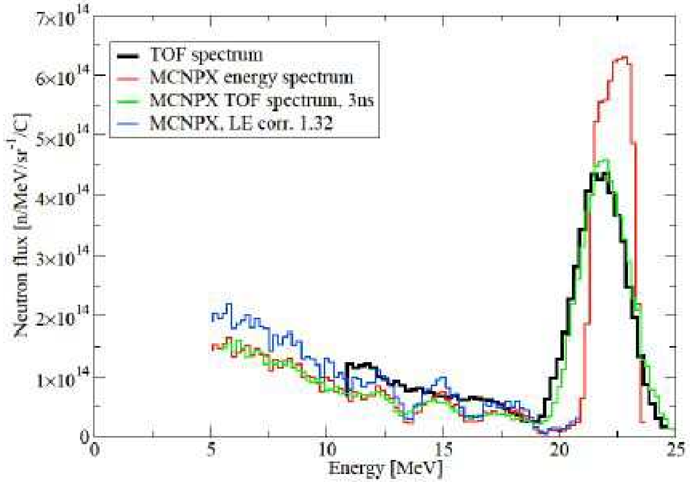

White neutron beam by Be (thick)

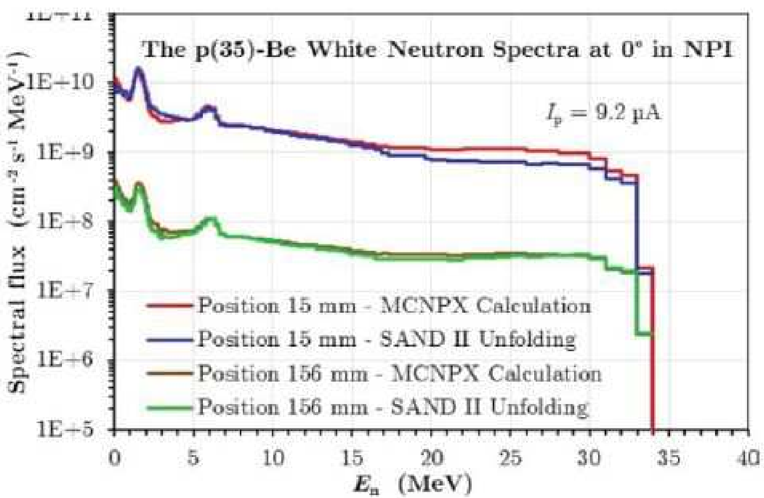

Online Monitoring of Neutrons

We are developing multichannel neutron fluence monitoring system for the online estimation of the neutron dose during the radiation hardness tests and CBM PSD operation including:

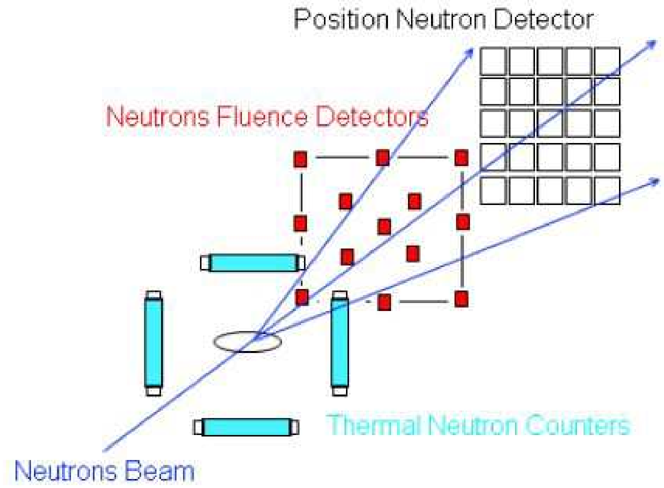

1. Neutron Fluence Detectors based on BPW34 pin diode

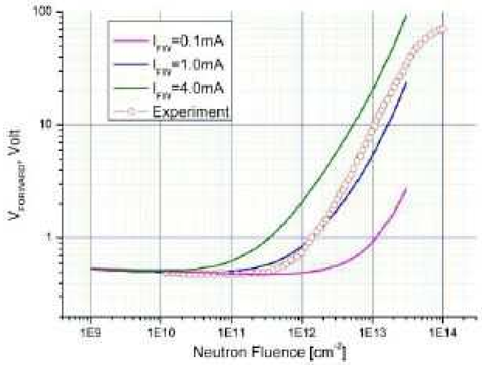

$V_{forward}$ ~ neutron fluence

2. Thermal Neutron Counters based on
- ZnS/LiF scintillators with high absorption of thermal neutrons
- SiPMs for light readout

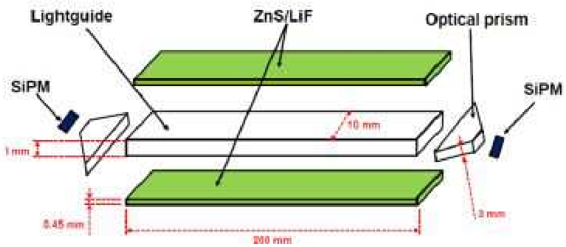

3. Position Neutron Detector based on plastic scintillators + SiPMs (JINR development)

Neutrons Fluence Detector (NFD)

Short theory – simulation

Using parameters of commercial PIN photo diode BPW34 to estimation influence of dose on each component of equation. Articles [1] & [2]

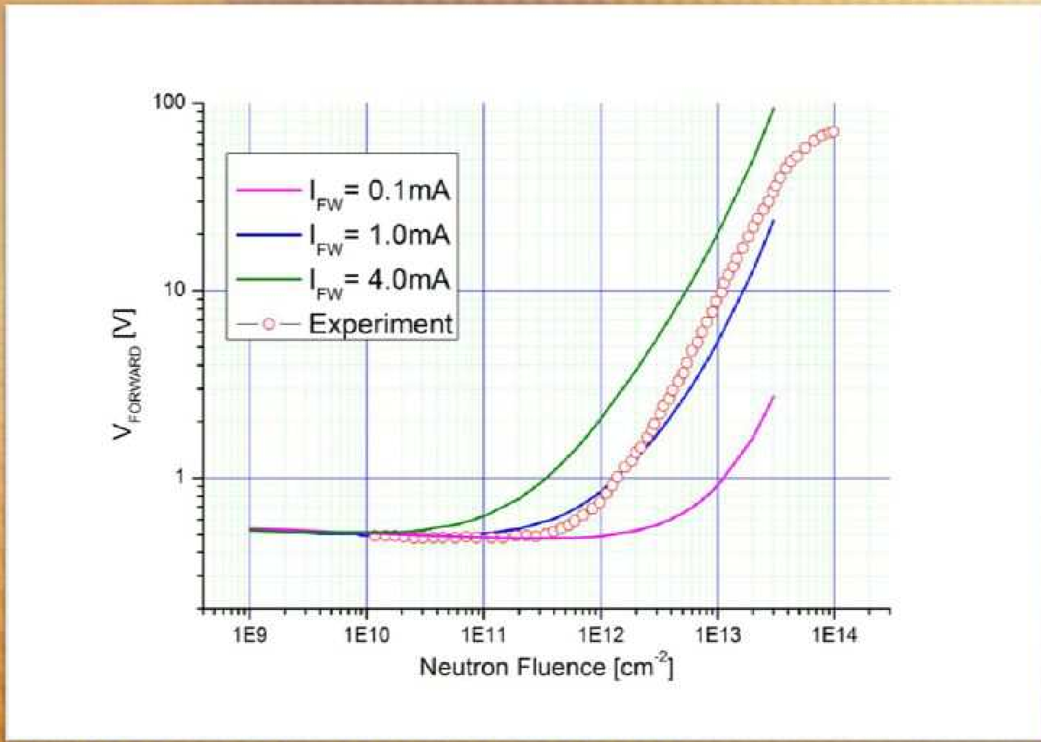

Graph 1: Experimental data for BPW34 from article [4] and results of simulation

NFD F-meter

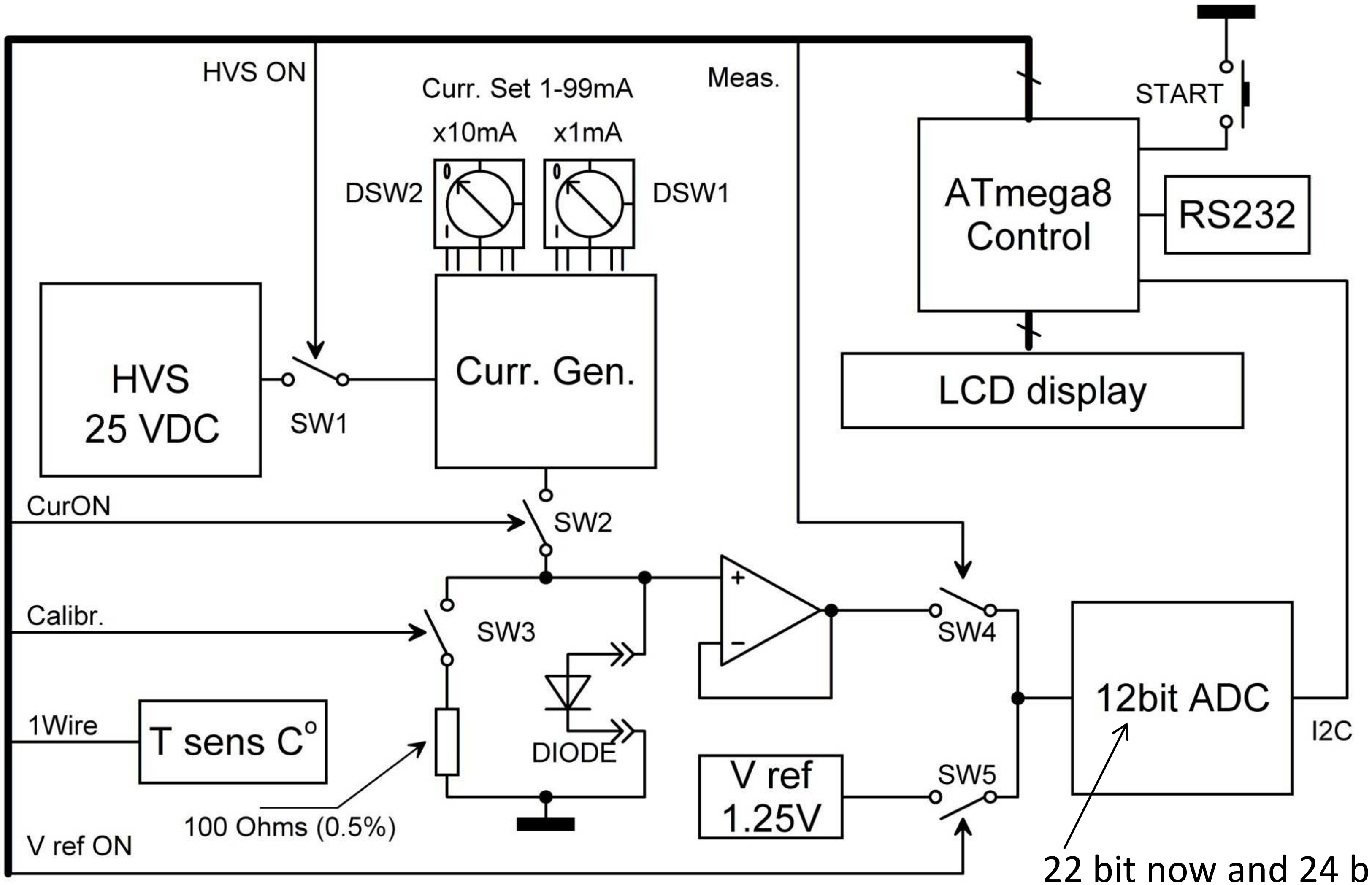

22 bit now and 24 bit for next prototype..

NFD test (2)

Experiment in November 2015 in NPI shown PIN sensor BPW34 sensitivity:

Forward voltage method - V_f/Φ_n~20 [uV/10E6 n/cm^2]

Transient charge method - Q_{trans}/Φ_n~0.04 [pCo/10E6 n/cm^2]

Experiment 21 September 2016 in NPI for calibration of 6xPIN sensors BPW34 in range: 0 up to 1E11 n/cm^2 have been carried out successful. Data analysis in progress..

Experimental Set-up

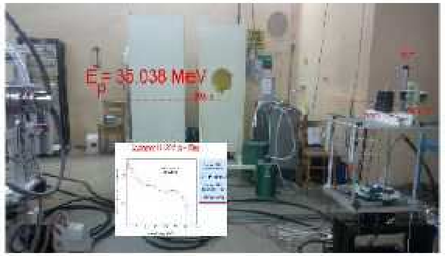

Test set-up for Ip=1uA, estimate F~5.04E5/1h

Calculation:

I_p, uA	Time, h	Dist.,m	F., [n/cm^2]
1	1	2	5.06E9
2	1	2	1.01E10
3	1	2	1.51E10
4	1	2	2.02E10
5	1	2	2.52E10

Test set-up for 2uA,3uA, 4uA, 5uA, 8u

Experimental results (V_{fw} and $I_{protons}$ vs time)

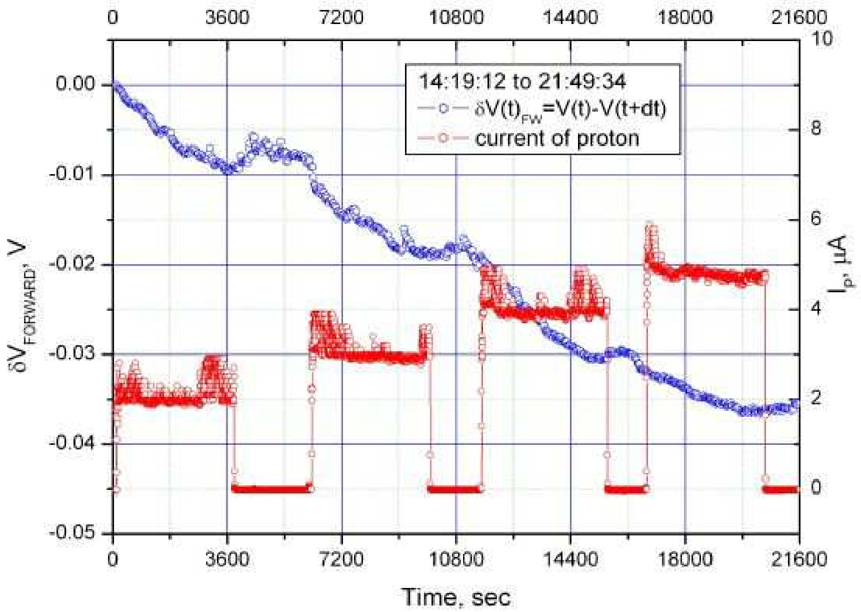

Thermal Neutron Counter (TNC)

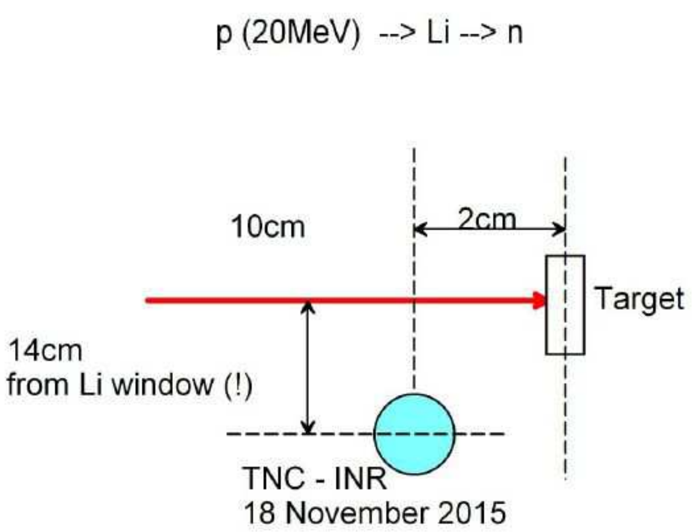

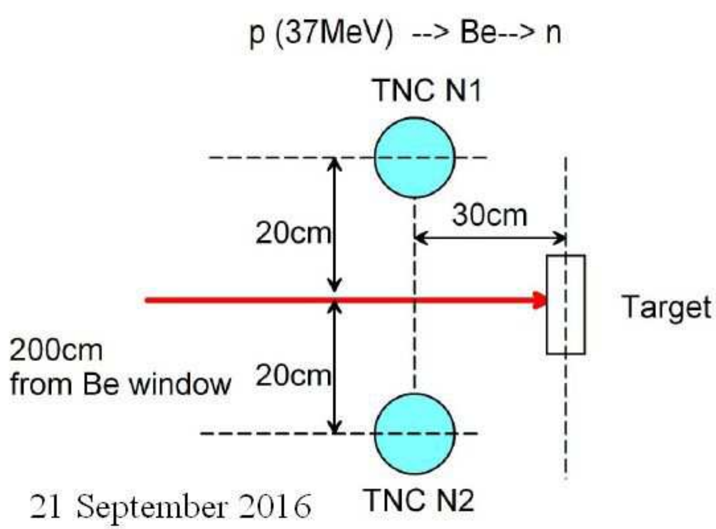

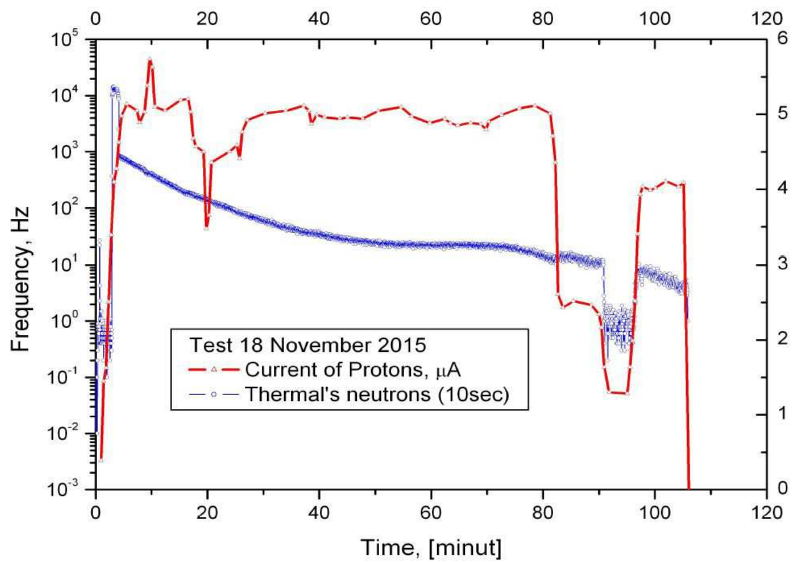

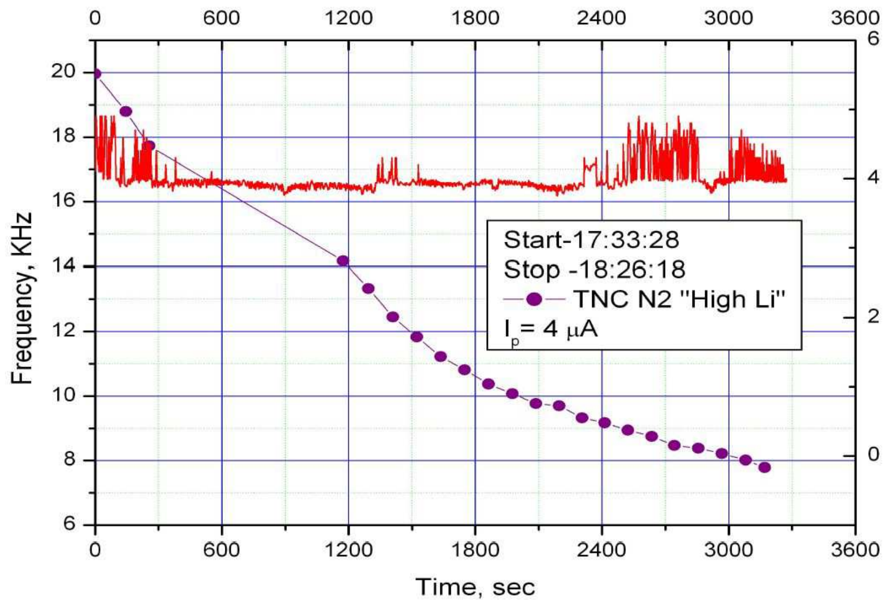

Position Neutron Detector (PND)

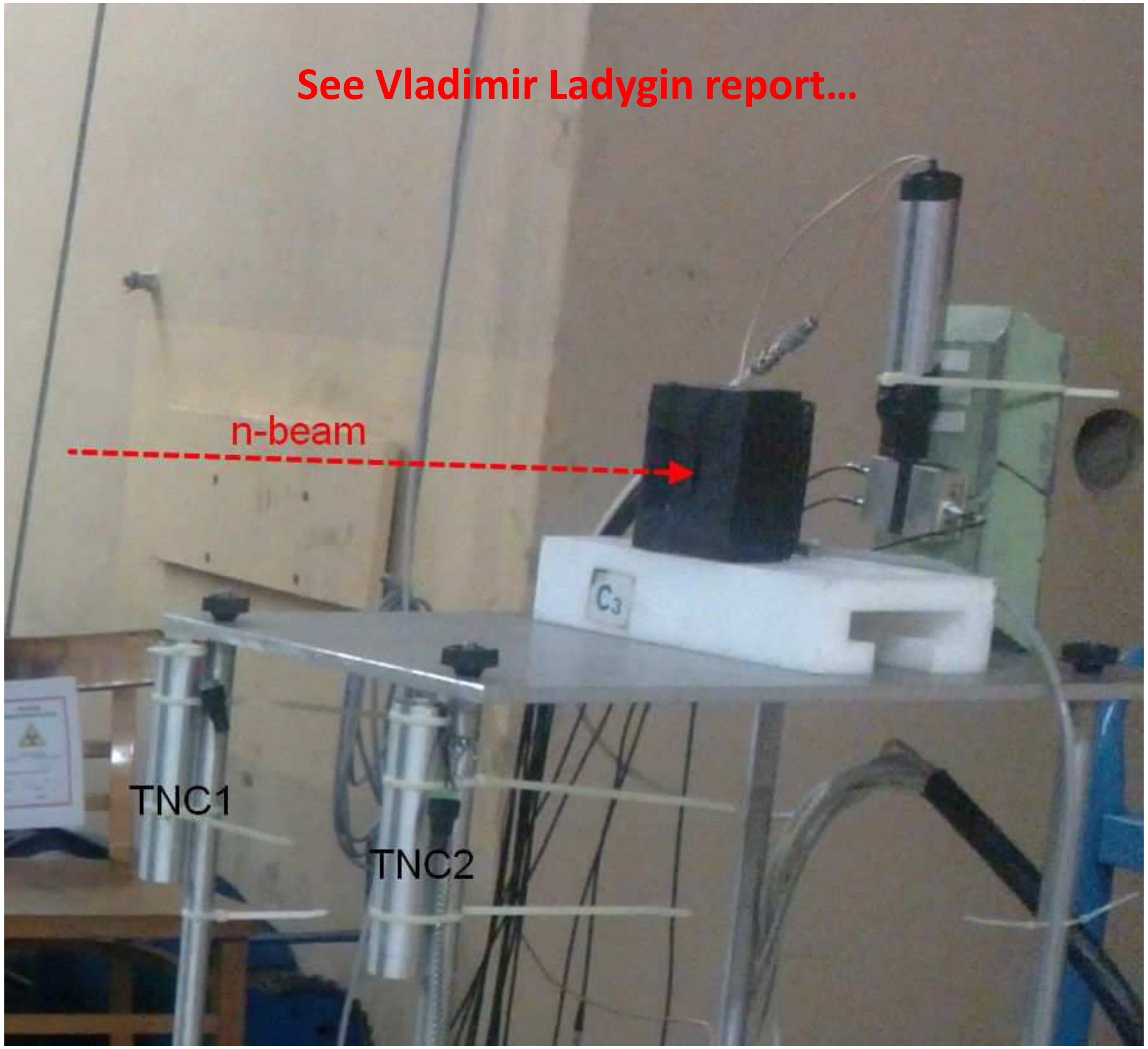

Next step – physics..

Methods of APD investigation

Static characteristics (C-V, C-F, I-F)

- investigation of internal structure of APD
- studying of the behaviors of impurities during APD operation
- measurement of the parameters of APD for equivalent circuit of APD in SPICE

Dynamic characteristics (transient effects)

- investigation of generation and recombination processes into APD bulk
- studying of noise sources behaviors of APD
- measurement of the parameters of noise sources for SPICE model of APD

Operation of APD

- single photon spectrum measurement with LED
- investigation of APD with scintillator and radioactive sources in laboratory
- investigation of APD with scintillator for cosmic rays

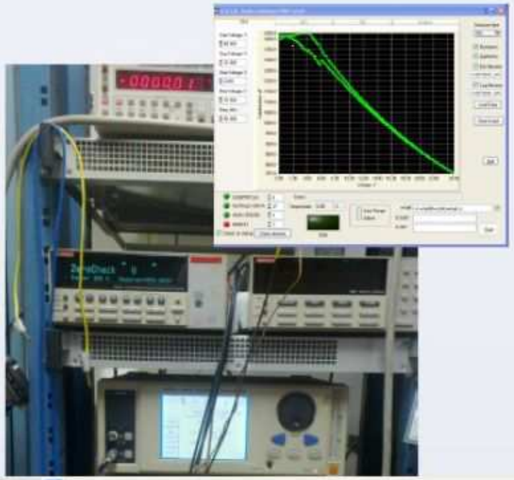

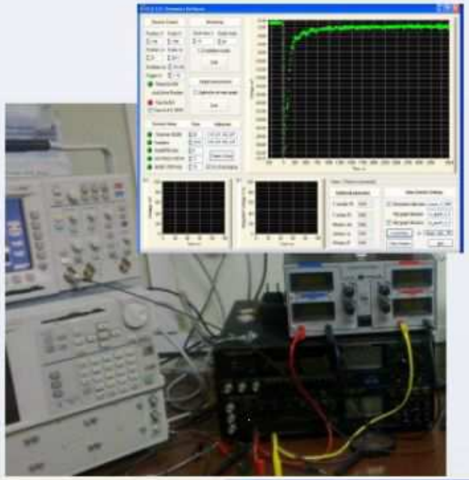

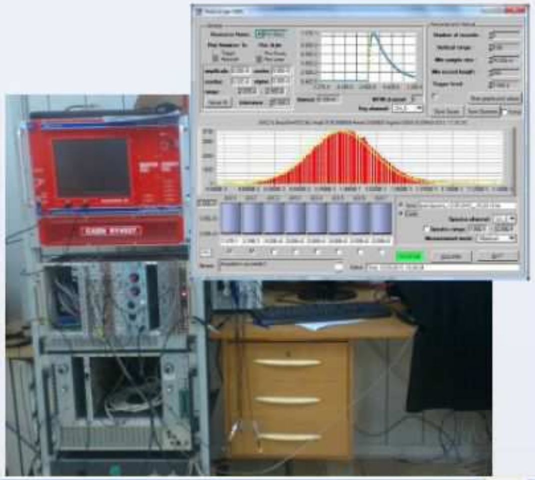

Conclusion and Plan

- Prototypes for all subsystem of common monitoring system tested and investigated;
- Next year we plan finish calibration of sensors and produce first 8 channel NFD module;
- System will integrated on software level and test in NPI (we have got permission for 5-6 experiment on cyclotron in NPI);
- We need to understand of problems with TNC;
- Beginning of work for investigation of changing structures of detectors during irradiation in online mode (fast I-V, C-V and C-F measurement during irradiation and calculation of profile P-N junction);

Thank you for attention!

Outlook

PIN theory (2)

Short theory – a bit of Maths

$$V_{FW} = \Phi_0(T)ln\left[\frac{I(t)N_d(\phi)}{eSN_i{}^2\sqrt{D_n\tau_n}}\right] + \Phi_0(T)ln\left[\frac{I(t)+B(N_t(\phi))}{A(N_d(\phi))-B(N_t(\phi))}\right] \quad \text{[eq.2]}$$

where $A(N_d(\phi)) = e\sqrt{\frac{D_n}{\tau_n(\phi)}}\frac{N_i{}^2}{N_{do}exp(-K_{nd}\phi)}$

and $B(N_t(\phi)) = e\frac{L}{2}N_iN_d exp(K_{nt}\phi)$

Heating process of diode: $\frac{dT}{dt} = \frac{\varrho_n(T)}{CpS^2}I(t)^2$ [eq.3]

After radiation the resistance of base increases in <u>k</u> times:

$$k = \frac{R_{Bi}}{R_{Bo}} = \cdots = \frac{\Delta T_1}{\Delta T_2} \quad \text{[eq.4]}$$

PIN theory (1)

Short theory – topology of PIN

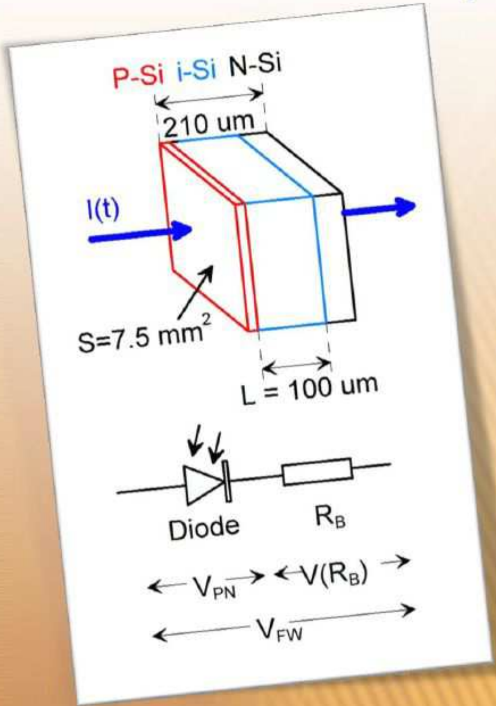

Figure 1: Diode BPW34 structure

Total forward voltage:

$$V_{FW} = V_{PN} + V_{RB} \qquad \text{[eq.1]}$$

According to work [1] and [2] we can present dependencies for each components of total voltage using the semiconductor's parameters as [eq.2]

SiPM P-N junction investigation (1)

KETEK

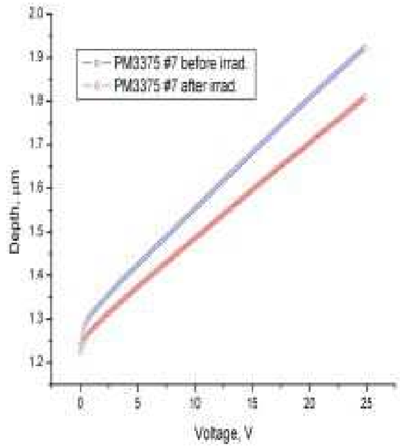

Fig. 2.1 Depletion width vs. V_{bias}

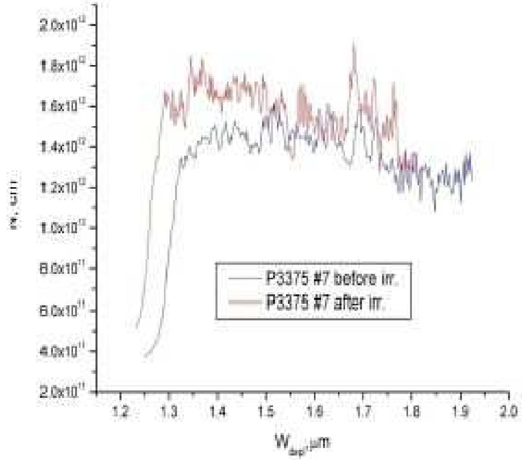

Fig. 2.2 Impurities produced in depletion region

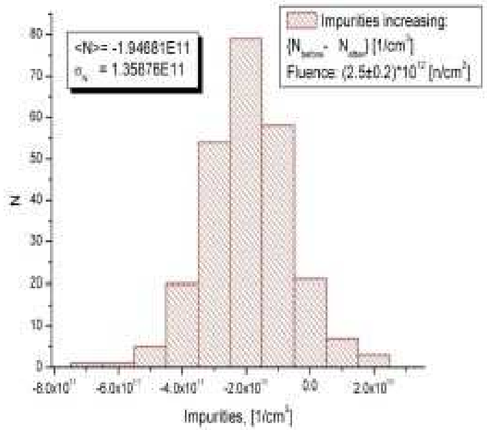

Fig. 2.3 The change of impurities after irradiation

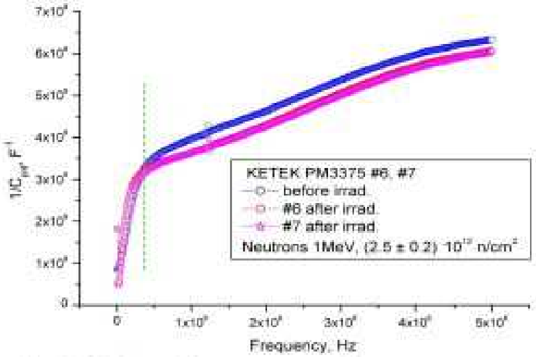

Fig. 2.4 Capacitance versus frequency

Internal resistance of KETEK SiPM decreases after irradiation that can be observed on Fig. 2.1 as depletion region shortening for the same voltages as before irradiation.

Generation–recombination noise $\delta\langle N_t^2\rangle$ depends on characteristics in Fig.2.4

$\delta\langle N_t^2\rangle/N_t \sim (4\tau_n/(1+(\omega\tau_n)))$; $\tau_n/N_t \sim 1/C(\omega)$; *where Nt - average number of carriers from traps,* τ_n *— carrier lifetime;* $\omega=2\pi f$; *f - frequency [12,13].*

Generation–recombination noise decreases for low frequency, but increases for high frequency.

We use KETEK SiPM for readout scintillator's hodoscopes during neutron beam test. Decrease of gain and increase of internal noise due to neutrons were observed. Hodoscope system was developed in JINR for position monitoring of neutron beam for Cyclotron U120 in NPI Rez.

SiPM P-N junction investigation (2)

SENSL SIPM

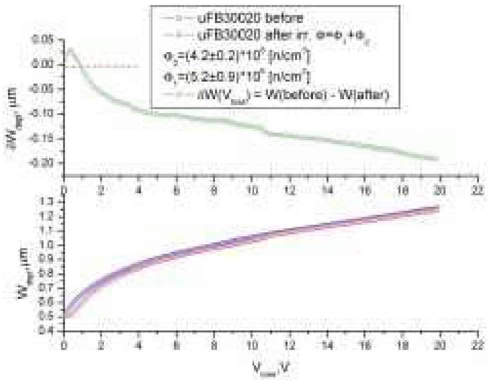

Fig. 4.1 Depletion width vs. V_{bias}

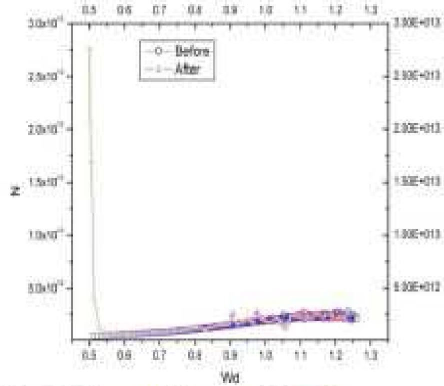

Fig. 4.2 Impurities produced in depletion region

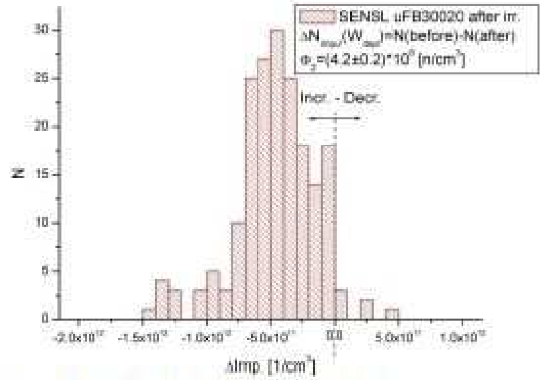

Fig. 4.3 The change of impurities after irradiation

SENSL compared to HAMAMATSU is more sensitive to irradiation in region near surface. Thermal neutrons flux was higher during irradiation of SENSL.

With help of neutron monitoring system calibrated for 1MeV neutrons, the part of thermal neutrons flux can be estimated.

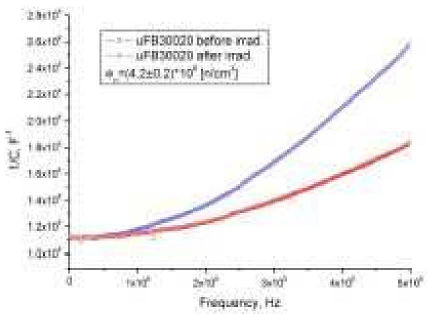

Fig. 4.4 Capacitance versus frequency

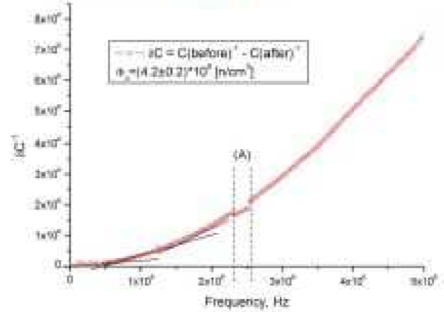

Fig. 4.5 Variation of capacitance before and after irradiation

Detector developed in JINR, Dubna was used for neutron monitoring. Generation–recombination noise increases homogeneity for all frequencies.

SiPM P-N junction investigation (3)

ZECOTEK

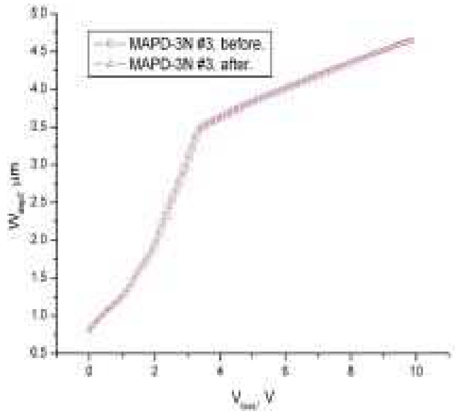

Fig. 3.1 Depletion width vs. V_{bias}

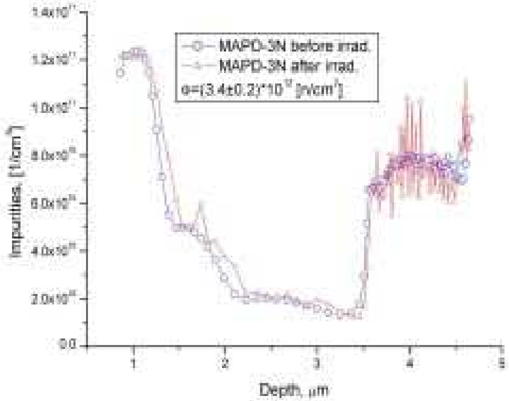

Fig. 3.2 Impurities produced in depletion region

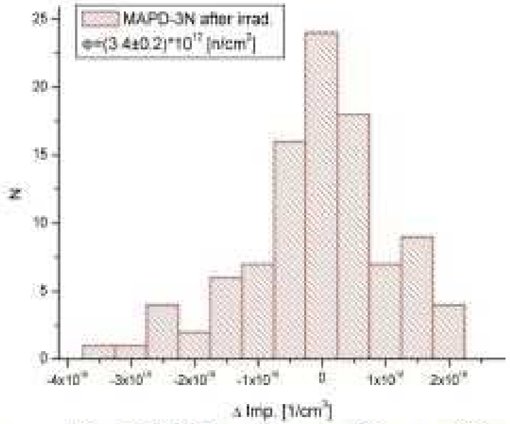

Fig. 3.3 The change of impurities after irradiation

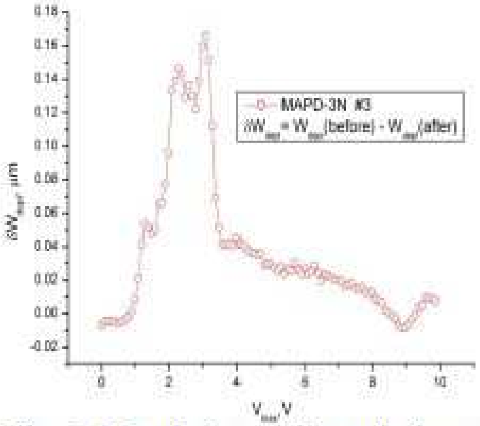

Fig. 3.4 Depletion width variation vs. V_{bias}

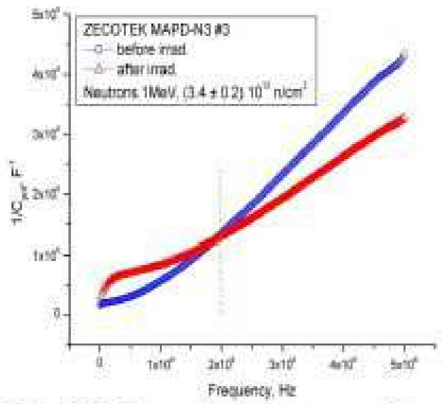

Fig. 3.5 Capacitance versus frequency

ZECOTEC has more symmetric change of impurities in depletion region. As a result, depletion region is more stable versus biasing voltage.

Generation–recombination noise $\delta\langle N_t^2\rangle$ increases for more high frequencies for ZECOTEK compared to KETEK.

SiPM P-N junction investigation (4)

HAMAMATSU

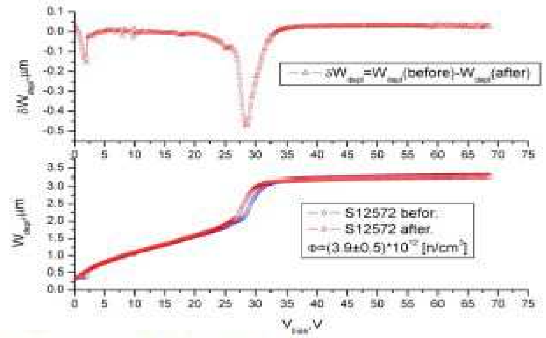

Fig. 1.1 Depletion width vs. V_{bias}

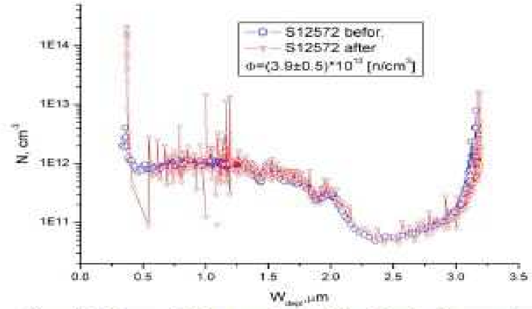

Fig. 1.2 Impurities produced in depletion region

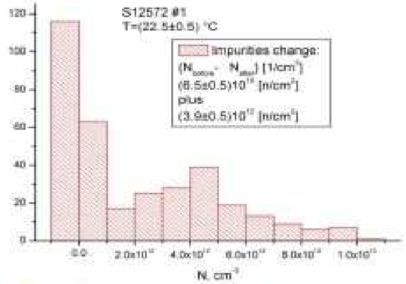

Fig. 1.3 The change of impurities after irradiation

Internal structure of HAMAMATSU changed more near surface, that can decrease sensitivity for blue light. Moreover, after irradiation detector is depleted for higher voltages. It can decrease sensitivity for light of long wavelength.

After first irradiation fife of tine to concentration ratio change not so strong as from beginning. Specific region from f_1 to f_2 was observed, where noise increase more than for other frequencies.

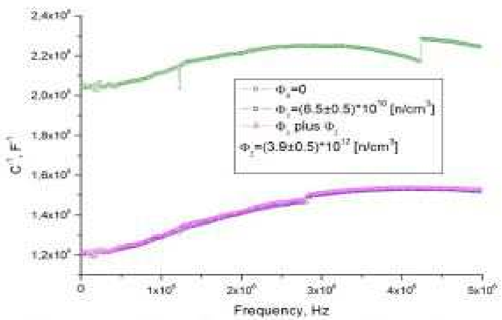

Fig. 1.4 Capacitance versus frequency

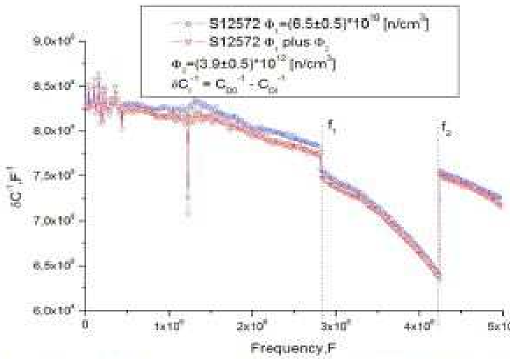

Fig. 1.5 Variation of capacitance before and after irradiation

AND more…

List of related publications

[1] V. Kushpil, V. Mikhaylov, S. Kushpil, P. Tlustý, O. Svoboda, A. Kugler, Radiation hardness investigation of avalanche photodiodes for the Projectile Spectator Detector readout at the Compressed Baryonic Matter experiment, Nuclear Instruments and Methods in Physics Research Section A, V. 787 July 2015, p. 117–120.

[2] S. Kushpil, V. Kushpil, V. Mikhaylov, Setup for laboratory studies of the environmental conditions influence on the fixed charge state in silicon dioxide, Journal of Instrumentation, V. 10 February 2015.

[3] V. Kushpil, V. Mikhaylov, A. Kugler, S. Kushpil, V.P. Ladygin, S.G. Reznikov, O. Svoboda, P. Tlustý, Neutron irradiation study of silicon photomultipliers from different vendors, Nuclear Instruments and Methods in Physics Research Section A, In Press, 2016.

[4] V. Mikhaylov, F. Guber, A.P. Ivashkin, A. Kugler, S. Kushpil, V. Kushpil, O. Svoboda, P. Tlusty, V.P. Ladygin, S. Seddiki and I. Selyuzhenkov, Performance of the forward calorimeters for heavy-ion experiments at FAIR, NICA, and CERN SPS, Proceedings of Science, PoS(EPS-HEP2015)281.

[5] V. Mikhaylov, A. Kugler, V. Kushpil, S. Kushpil, O. Svoboda, P. Tlusty and V.P. Ladygin, Radiation hardness tests of Avalanche Photodiodes for FAIR, NICA, and CERN SPS experiments, Proceedings of Science, PoS(EPS-HEP2015)282.

[6] V. Kushpil, V. Mikhaylov, S. Kushpil, O. Svoboda, P. Tlustý, A. Kugler, Investigation of avalanche photo diodes in NPI Rez in frame of collaboration work with JINR in 2014, PoS (Baldin ISHEPP XXII), 2015.